ARTICLE
Journal of Cellular Biochemistry 105:277–289 (2008)

Journal of Cellular Biochemistry

Increased Hepatic UCP2 Expression in Rats With Nonalcoholic Steatohepatitis Is Associated With Upregulation of Sp1 Binding to Its Motif Within the Proximal Promoter Region

Ying Jiang,[1] Hua Zhang,[2] Ling-yue Dong,[1] Dan Wang,[2] and Wei An[1*]

[1] *Department of Cell Biology and Municipal Laboratory for Liver Protection and Regulation of Regeneration, Capital Medical University, 100069 Beijing, China*

[2] *Department of Anatomy and Histology, Capital Medical University, 100069 Beijing, China*

ABSTRACT

Uncoupling protein-2 (UCP2) is a mitochondrial inner-membrane carrier protein that is involved in the control of fatty acid metabolism. To understand the mechanism of the transcriptional regulation of *ucp2* in the pathogenesis of nonalcoholic steatohepatitis (NASH), we cloned 500 bp upstream of the *ucp2* exon 1 from a rat liver cDNA library and identified *cis*-acting regulatory elements. The transcriptional start site was identified as "C," −359 bp from the ATG codon. A reporter gene assay showed that deletion of the nucleotide sequence between −264 and −60 bp resulted in a significant decrease in promoter activity in HepG2 and H4IIE cells. Electrophoretic mobility shift assay (EMSA) and chromatin immunoprecipitation (ChIP) revealed that the increase in promoter activity is related to an enhanced ability of Sp1 to bind to its motifs at −84 to −61 bp within the *ucp2* proximal promoter. Overexpression of exogenous Sp1 in H4IIE cells also increased the promoter activity. We demonstrated that the expression of UCP2 mRNA and protein is markedly increased in rats with nonalcoholic steatohepatitis (NASH). Coincidently, levels of Sp1 binding to −84/−61 bp were also increased. Overall, our data indicate that the Sp1-binding site located at the proximal promoter is involved in the regulation of rat UCP2 expression. J. Cell. Biochem. 105: 277–289, 2008.

KEY WORDS: UNCOUPLING PROTEIN-2; PROMOTER; TRANSCRIPTION; Sp1; NONALCOHOLIC STEATOHEPATITIS

Nonalcoholic fatty liver disease (NAFLD) is a chronic disease with a spectrum of hepatic pathology such as simple steatosis, steatohepatitis [also known as nonalcoholic steatohepatitis (NASH)], fibrosis and cirrhosis [Ludwig et al., 1980; Clark et al., 2002]. Steatosis is usually considered to be benign, but NASH is increasingly acknowledged as being a precursor to more severe liver disease, and sometimes evolves into "cryptogenic" cirrhosis [Caldwell et al., 1999; Neuschwander-Tetri and Caldwell, 2003]. NASH is a clinically important type of chronic liver disease in industrialized countries and, in addition, rates are increasing in developing countries. The mechanisms that lead to NASH are unclear, although it is thought to arise from the interaction of many different genes and lifestyle factors. Mitochondrial impairment, oxidative stress and metabolic deregulation have all been implicated in the pathogenesis of steatohepatitis [Day, 2002; Farrell et al., 2007].

Uncoupling protein-2 (UCP2) is a mitochondrial inner-membrane carrier protein. As their name indicates, uncoupling proteins (UCPs) serve an uncoupling function, specifically by uncoupling mitochondrial electron transport from ATP synthesis. Genetic

Abbreviations used: UCP2, uncoupling protein-2; NASH, nonalcoholic steatohepatitis; NAFLD, nonalcoholic fatty liver disease; EMSA, electrophoretic mobility shift assay, ChIP, chromatin immunoprecipitation; SREBP-1c, sterol-regulatory-element binding protein-1c; ECL, enhanced chemiluminescence; ALT, alanine aminotransferase; AST, aspartic aminotransferase; GLU, glucose; TC, total cholesterol; TG, triglyceride; LDL, low density lipoprotein; HDL, high density lipoprotein; 5′-RACE, 5′-rapid amplification of cDNA ends; FLA, firefly luciferase activity; RLA, renilla luciferase activity; TSS, transcriptional start site.

Grant sponsor: National Natural Science Foundation of China; Grant number: 30470643; Grant sponsor: National "863" Project; Grant number: 2006AA02A410; Grant sponsor: Beijing Municipal Commission of Education.

*Correspondence to: Dr. Wei An, Department of Cell Biology and Municipal Laboratory for Liver Protection and Regulation of Regeneration, Capital Medical University, 10 You An Men Wai Xi Tou Tiao, Beijing 100069, China. E-mail: anwei@ccmu.edu.cn

Received 12 December 2007; Accepted 28 April 2008 • DOI 10.1002/jcb.21827 • 2008 Wiley-Liss, Inc.

Published online 9 June 2008 in Wiley InterScience (www.interscience.wiley.com).

studies have shown that the gene *ucp2* is mapped to the chromosome region 1q33 in rats [Kaisaki et al., 1998]. The *ucp2* mRNA is transcribed from the distal six of eight existing exons of *ucp2* [Fleury et al., 1997; Ricquier and Bouillaud, 1997]. Rat UCP2 protein comprises 309 amino acids, has a molecular mass of 33 kDa and shares 99% and 95% homology to mouse and human UCP2, respectively [Matsuda et al., 1997; Tu et al., 1998; Pecqueur et al., 1999]. The *ucp2* mRNA has been detected in many tissues in humans and rodents, and the ubiquitous expression of *ucp2* indicates that the protein may be important. Genetic studies have indicated that the *ucp2* gene is localized in the proximity of a cluster of five genes related to energy homeostasis and obesity [Fleury et al., 1997; Ricquier and Bouillaud, 1997]. Therefore, *ucp2* might be theoretically linked to hyperinsulinemia or to the resting metabolic rate and, consequently, to the control of body weight. It has also been proposed that UCP2 contributes to the inflammatory response and regulates the production of reactive oxygen species in mitochondria [Pecqueur et al., 2001].

The relationship between UCP2 and NAFLD seems to be more than serendipitous. In line with the ''two-hit'' theory of NAFLD progression, it seems more feasible that UCP2 contributes to the transition of steatosis into steatohepatitis. UCP2 has the ability to affect hepatocellular bioenergetics upon additional challenges. Under normal conditions, the level of *ucp2* mRNA expression in hepatocytes is very low or undetectable [Larrouy et al., 1997], but in the livers of fa/fa rats or rats fed a high-fat diet the levels of UCP2 protein and mRNA were increased [Matsuda et al., 1997; Hidaka et al., 1998]. UCP2 also enhances fat accumulation in the liver and increases insulin resistance, resulting in increased levels of plasma fatty acid and various fat-derived bioactive factors [Baffy, 2005]. Recently, the concept that NASH is a form of mitochondrial disease has become more acceptable [Fromenty et al., 2004; Pessayre and Fromenty, 2005]. However, it is unclear how *ucp2* gene transcription is controlled, in addition to its relationship to the pathobiology of NASH. The *ucp2* gene is under strict transcriptional control, and can be regulated by inflammation, leptin and peroxisome proliferator-activated receptor γ (PPARγ) agonists [Baffy, 2005].

The *ucp2* mRNA in hepatocytes is upregulated by the stimulation of bacterial lipopolysaccharide and is overexpressed in genetically modified *ob*/*ob* mice [Cortez-Pinto et al., 1998]. It has been shown that the proximal promoter of the mouse *ucp2* gene contains potential binding sites for sterol-regulatory-element binding protein-1c (SREBP-1c), E box and Sp1, in addition to liver X receptor. In HIB-1B pre-adipocytes and islet INS-1 β-cells, *ucp2* transcription can be enhanced by increasing binding to SRE, E box and Sp1, or by the addition of PPARγ [Medvedev et al., 2001, 2002].

The aim of the present study was to observe the hepatic expression of UCP2 in rats with NASH. Transcriptional characteristics of the rat *ucp2* promoter were identified using a gene reporter assay. A *cis*-element Sp1 in the proximal promoter was found to be essential for governing *ucp2* transcription. Moreover, the relationship between UCP2 expression and Sp1 binding was clearly demonstrated in rats with NASH. We conclude that UCP2 expression in the livers of rats with NASH is attributable to the regulation of Sp1 binding to the *ucp2* proximal promoter.

MATERIALS AND METHODS

MATERIALS

HepG2 and H4IIE cells (rat hepatoma) were obtained from American Type Culture Collection (ATCC). Marathon-ready rat liver cDNA was purchased from Clontech Company (USA). RNA extraction kit using Trizol reagent and pBlue-TOPO TA vector were products of Invitrogen Company (USA). For DNA cloning, TA vector was obtained as pMD18-T vector from TaKaRa Company (Japan). For the promoter assay, pGL3-Basic luciferase vector, its control vector pRL-TK and DNA transfection agent Tfx-20 were obtained from Promega Company (USA). The chemiluminescent EMSA assay kit was obtained from Pierce Company (USA). The ChIP assay kit was a product of Upstate (USA). Primary antibody against UCP2 and enhanced chemiluminescence (ECL) kit were manufactured by Santa Cruz Company (USA). The SYBR Green PCR assay kit for real-time PCR analysis was from Applied Biosystems Company (USA).

ANIMALS

Male Sprague-Dawley rats (110–130 g) were caged, maintained on a 12:12-h light–dark cycle at 22–25°C and allowed free access to water during all stages of the study. Food intake and body mass were recorded. All protocols for animal care and experiments were approved by the Ethical Committee of Capital Medical University Beijing. The animals in the control group were fed a standard diet (5% of energy derived from fat, 23% from protein, 55% from carbohydrate, 6% from fibrate, 1.2% from calcium, 0.8% from phosphorus and 9% from water) with ad libitum food intake, whereas the rats in the NASH group were fed a high-fat diet (88% standard diet plus 2% cholesterol and 10% lard) with ad libitum food intake. All animals were fed between 8 am and 9 am each day.

After the 12-week dietary intervention period, the rats were killed by puncture of the abdominal aorta after overnight fasting, and the livers were removed rapidly, weighed and dissected. Blood glucose (GLU), total cholesterol (TC), triglyceride (TG), low density lipoprotein (LDL), and high density lipoprotein (HDL) levels were measured. Serum activities of the liver-associated enzymes alanine aminotransferase (ALT) and aspartic aminotransferase (AST) were determined using an autoanalyzer in the Clinical Chemistry Laboratory of the Youan Hospital, Capital Medical University Beijing. Partial liver specimens were snap frozen in liquid nitrogen and stored at −80°C for subsequent analysis. Formalin-fixed and paraffin-embedded livers were processed routinely for hematoxylin–eosin staining and Masson's staining. Sections of frozen rat liver tissue were stained with oil red O for hepatic lipid droplets. Tissues samples were placed into 2.5% buffered glutaraldehyde, processed into resin, and cut for transmission electron microscopy. The histology results were analyzed by a pathologist who was unaware of animal grouping.

IDENTIFICATION OF THE INITIATION OF RAT *ucp2* TRANSCRIPTION

To elucidate the regulatory elements of *ucp2*, the transcription start site was determined by amplifying Marathon-ready rat liver cDNA with 5′-rapid amplification of cDNA ends (5′-RACE). All of the primers employed in 5′-RACE are shown in the Table I. Adapter primer (AP) 1 and gene-specific primer (GSP)1 were applied in the

TABLE I. Oligonucleotide Sequences

Oligos	Sequence (5′–3′)	Position (bp)	Comments
AP1-F	CCATCCTAATACGACTCACTATAGGGC		Invitrogen Company
GSP1-R	GAAGGAAGGCATGAACCCCTTGTAG	1,150–1,175	RACE primers (from exon 1)
AP2-F	ACTCACTATAGGGCTCGAGCGGC		Invitrogen Company
GSP2-R	GTGCAATGGTCTTGTAGGCTTCGAC	821–846	RACE primers (from exon 1)
P960-F	AGCAGCCCAAACCCACTTGAGCTTCTATTA	−868 to −838	Promoter deletion primers (from +1)
P960-R	AGGAGAATACACAGGAGAACACAGGAGTGC	63–93	
P458-*Kpn*I-F	CATGGTACCGCAGAGGGAAGGTGAGGC	−458 to −441	
P264-*Kpn*I-F	CATGGTACCCAGGGCAGGGTAGGAAGT	−264 to −247	
P60-*Kpn*I-F	CATGGTACCGACCACGCCCGCCAGACT	−60 to −43	
P-*Nhe*I-R	TCAGCTAGCATACACAGGAGAACACAG	70–87	
E-Bio-F	TCCCGCCTCTTCACGCCACGCCCC-Bio	−84 to −61	EMSA primers (from +1)
E-F	TCCCGCCTCTTCACGCCACGCCCC	−84 to −61	
E-R	GGGGCGTGGCGTGAAGAGGCGGGA	−84 to −61	
mE-F	TCCTACCTCTTCACGCCACGCCCC	−84 to −61	
mE-R	GGGGCGTGGCGTGAAGAGGTAGGA	−84 to −61	
UCP2-F	GAGAGTCAAGGGCTAGCGC	479–498	Real-time RT-PCR primers (from exon1)
UCP2-R	GCTTCGACAGTGCTCTGGTA	809–829	
β-Actin-F	ACCCACACTGTGCCCATCTA		
β-Actin-R	GCCACAGGATTCCATACCCA		
β-Actin-F	AACCCTAAGGCCAACCGTGAAAAG		RT-PCR primers
β-Actin-R	TCATGAGGTAGTCTGTCAGGT		
p149-F	ACAGATGGAAACGCCTCCTCACC	−128 to −106	Real-time CHIP-PCR primers (from +1)
p149-R	AGCGATCCCAGGGCACCGA	3–21	
p actin-F	CGCCGTTCCGAAAGTTGCC	−78 to −60	CHIP-PCR β-actin primers (from exon1) (negative control)
p actin-R	AAGGTTGTACTCGCGGGTGG	16–37	

first round of PCR. In the second round, AP2 and the upstream internal GSP2 were used. After two rounds of amplification, a major RACE product (~900 bp) was obtained, subcloned into TA pMD18-T vector and verified using DNA sequencing. The transcription initiation site was determined using sequence analysis in five independent clones, and was defined as +1.

CONSTRUCTION OF RAT *ucp2* PROMOTER LUCIFERASE PLASMIDS

A DNA fragment of *ucp2* promoter region from position −868 to position +93 was amplified by PCR, using rat genomic DNA as a template. The positive PCR product was ligated into pBlue-TOPO TA vector and verified using DNA sequencing. Subsequently, this 961-bp fragment was used as the template for promoter deletion assay of *ucp2*. The deletions were generated by PCR, using a primer targeted on exon 1 at the 3′ end of *ucp2*, and three 5′ primers complementary to nucleotides −458 to +87, −264 to +87, and −60 to +87 bp. These constructs were nominated p458, p264, and p60, respectively. These fragments (−458 to +87, −264 to +87, and −60 to +87 bp) were inserted into *Kpn*I (upstream) and *Nhe*I (downstream) of the pGL3-Basic luciferase vector, respectively, forming three *ucp2* promoter deletion constructs (pGL3-p458, pGL3-p264, and pGL3-p60) for further assay. All of the primers used in the construction of the deleted promoter are listed in Table I.

TRANSIENT TRANSFECTION AND PROMOTER ACTIVITY ASSAY

To identify the promoter elements that govern the transcriptional activity of *ucp2*, the gene promoter deletion constructs were transiently transfected in H4IIE and HepG2 cells by using DNA transfection agent Tfx-20.

The cells of 80% confluence (~1×10^4 cells per well) were co-transfected with 0.3 μg of one of the pGL3-*ucp2* promoter constructs and 0.03 μg of pRL-TK vector, which expresses Renilla luciferase under the control of the TK promoter and reflects the efficiency of DNA transfection. The transfection procedures were performed following previous description [Samaras et al., 2002]. Subsequently, the cells were lyzed and the luciferase activity was measured using a luminometer equipped with a dual reporter assay system (Promega Company). The activity (FLA/RLA) of the promoterless vector pGL3-Basic was taken as control.

ELECTROPHORETIC MOBILITY SHIFT ASSAY

Nuclear extracts of H4IIE cells and rat liver samples were prepared with the nuclear extraction reagents kit (Pierce Company). The protein concentration was determined by the method of Lowry [Lowry et al., 1951]. The probes (Table I) and experimental procedures were followed as per product instruction. All of the reaction mixture [20 fM labeled probe with nuclear extract (5 μg) and competing oligonucleotides (4 pM) in binding buffer] was incubated at room temperature for 30 min. Electrophoretic mobility shift assays (EMSA) were performed using size fractionation of the reaction mixture on a non-denaturing 6% polyacrylamide gel containing 0.5× TBE buffer. Following gel separation, DNA/protein complexes were transferred to a nylon membrane and detected using an enhanced chemiluminescence assay for biotin-labeled probes [Sauzeau et al., 2003].Where supershift assays were performed, 2 μg of polyclonal anti-Sp1 antibody was added to nuclear extracts and incubated on ice for 20 min prior to addition of the labeled probe.

CHROMATIN IMMUNOPRECIPITATION ASSAY (CHIP)

H4IIE nuclear extract was used to perform the ChIP assay according to the instructions of the ChIP assay kit. 1×10^6 cells or liver pieces were fixed with 1% formaldehyde for 10 min at room temperature [Gummow et al., 2003; Lagor et al., 2005]. An aliquot of the supernatant was saved as total input chromatin. Anti-Sp1 polyclonal antibodies (4 μg) were used for immunoprecipitation. As an internal control, an aliquot of anti-Sp1-pulldown chromatin

and the input chromatin were amplified in parallel using primers for the β-actin gene promoter (namely, p-actin, Table I), which is not a target of Sp1 [Chakravarty et al., 2004; Rubio et al., 2007]. As a negative control, normal rabbit immunoglobulin G (IgG) was used. The reaction in which no primary antibody added was used as a blank control. Finally, nuclear DNA extracts (with or without antibody) were amplified using primers that spanned the Sp1 region of the *ucp2* promoter (from −264 to +87 bp). The amplified DNA fragments were separated by electrophoresis using 2% agarose gels and stained with ethidium bromide.

For relative quantification of PCR reactions, ChIP DNA was also subjected to quantitative real-time PCR assay using SYBR Green dye and an ABI-7300 PCR system, according to the manufacturer's protocol (ABI). The input and Sp1-ChIP DNAs were amplified in triplicate under the following conditions: 50°C for 2 min, 95°C for 10 min, 40 cycles at 95°C for 15 s, and 60°C for 1 min. The relative differences between input sample and Sp1-ChIP product or negative control were determined using the ΔCT method [Ou et al., 2004] and presented as the percentage of the input, which was taken as 100%. Data are the mean ± SD from triplicate samples of three independent experiments. PCR amplification of *ucp2* was performed with primer 149 (−128/+21, namely p149). The specificity of p149 was established using dissociation curves.

DETECTION OF HEPATIC UCP2 EXPRESSION

Real-time PCR was performed to analyze the expression of *ucp2* mRNA [Schmittgen et al., 2000]. Total hepatic RNA from a liver tissue sample was extracted using Trizol reagent, and reversely transcribed into cDNA using Superscript III reverse transcriptase (Invitrogen Company) according to procedures described previously. Quantitative real-time PCR assays were performed in the presence of the oligonucleotide primers for *ucp2* and quantified using SYBR Green PCR reagents. Rat β-actin was used as an internal control for this method, with each sample determination carried out in triplicate. The parameters for real-time PCR were similar to that described in Chromatin Immunoprecipitation Assay (ChIP) Section.

Western blot assays were used to analyze UCP2 protein expression [Pecqueur et al., 2001]. Total cellular protein from frozen rat liver tissue was extracted by homogenizing the sample in a buffer containing 10-mM Tris–HCl (pH 7.6), 5-mM EDTA, 50-mM NaCl, 1% Triton X-100, 1-μg/ml leupeptin, 1-μg/ml aprotinin, 0.1-μM phenylmethylsulfonyl fluoride and 50-mM NaF. The homogenate was then centrifuged at 12,000*g* for 15 min at 4°C and supernatants were collected. One hundred micrograms of cellular extracts were separated by 12.5% SDS–polyacrylamide gel and electrotransferred onto nitrocellulose membranes. The membranes were incubated with goat anti-human UCP2 polyclonal antibody as the primary antibody (1:200), and then with horseradish peroxidase conjugated to rabbit anti-goat IgG as the second antibody (1:2,500). The positive reaction against UCP2 antibody was visualized using ECL reagent, followed by exposure to Kodak X-Omat X-ray film.

To verify Western blot detection, UCP2 expression in the liver was immunohistochemically analyzed. Formalin-fixed, paraffin-embedded tissue of rat liver was performed as routine. Paraffin-embedded tissue specimens were deparaffinized, rehydrated and endogenously blocked. Subsequently, antigens in slides were retrieved as follows. Briefly, the slides were placed in a plastic coplin jar filled with 0.01 M citrate buffer and subjected to microwave treatment at medium power for 5–10 min. To compensate for evaporation, the buffer was refilled and the process was repeated. The slides were blocked with 10% goat serum for 30 min at room temperature and incubated (12 h at 4°C) with a rat polyclonal antibody of UCP2 [(1:100), Boster Company, Beijing]. The slides were incubated with secondary antibody (goat anti-rat IgG labeled with biotin), and positive cells were visualized with diaminobenzidine (DAB).

STATISTICS

Data are expressed as means ± SD. Statistical analysis was performed using one-way analysis of variance (ANOVA). Differences were considered to be significant when $P < 0.05$.

RESULTS

IDENTIFICATION OF THE TRANSCRIPTIONAL START SITE OF RAT *ucp2*

5′-RACE, which is widely used as an alternative strategy for detecting the transcriptional initiation of genes, enabled the capture of extra 5′-sequences to compensate for those lost during the construction of the conventional cDNA library. To elucidate the regulatory role of *ucp2* in the pathogenesis of NASH, the transcription initiation site was determined by 5′-RACE, using Marathon-ready cDNA as the template with the adaptor primer and the *ucp2*-specific primer that binds from 821 to 846 bp and from 1,150 to 1,175 bp distal to *ucp2* exon 1 (Fig. 1A). 5′-RACE was carried out for three separate cDNA libraries. For each cDNA library, 5′-RACE products were amplified using the pair primers of AP1-GSP1 and AP2-GSP2. Figure 1B shows PCR amplification of the cDNA library in combination with two pairs of primers. The products from 15 different 5′-RACE reactions were sequenced. The longest transcript identified contained 359 bp 5′-upstream of the start codon ATG, indicating that this "C" (denoted by an asterisk in Fig. 1C) represents the potential transcription initiation site, denoted by +1.

After identification of the start site of *ucp2* transcription, the sequences of rat *ucp2* promoter region between −868 and +93 bp were analyzed. Using computer-assisted sequence alignment, it was observed that the rat *ucp2* promoter contained neither a typical TATA box nor a typical CAAT box; instead, abundant GC-rich elements comprising several Sp1-, SRE-, E-box-, and AP4-binding sites were found in the proximal region of the promoter.

ACTIVITY ASSAY OF THE RAT *ucp2* PROMOTER

For analysis of the rat *ucp2* promoter activity, three promoter deletion constructs were generated by PCR and the promoter activities were determined. Three fragments of the promoter with different lengths—nominated P458, P264, and P60—were fused to the promoterless vector PGL3-Basic. The resultant three promoter constructs were then transiently transfected into rat and human liver-originated cell lines (H4IIE and HepG2 cells), respectively. Promoter activities in both cell lines were measured using a luminometer equipped with dual reporter assay system. Even the promoter fragment P60 (−60 to +87 bp) exhibited luciferase activity

Fig. 1. Identification of rat *ucp2* transcriptional start site (TSS). A: Schematic drawing of rat *ucp2* structure and 5′-RACE. B: 5′-RACE product obtained using marathon-ready cDNA library from rat liver with primer GSP2 (Table I). Arrowhead indicated a 5′-RACE product. The transcriptional start site was identified by sequence alignment and was mapped at 359 bp upstream of the sequence in GenBank (accession no. AB010743). C: Partial sequences of the rat *ucp2* promoter. The transcription start site is indicated by an asterisk (designated +1). The deduced putative binding sites for transcription factors are underlined.

that was at least 10-fold that of the promoterless construct (PGL3-Basic) in two cell lines, implying that this region could be regarded as a minimal promoter of *ucp2* (Fig. 2A). Another two constructs, P264 (−264 to +87 bp) and P458 (−458 to +87 bp), also had a dominant role in controlling promoter activity. In HepG2 and H4IIE cells, the promoter spanning −264 to −60 bp had an important role in maintaining activity because deletion of this fragment led to a marked decrease in luciferase activity. Furthermore, a reduction in luciferase activity in H4IIE cells was observed after deletion of the region −458 to −264 bp, indicating that there are functionally positive *cis*-acting elements in these regions. We checked these experimental data further using TRANSFAC 5.0 software, and the result indicated that several important *cis*-acting elements such as Sp1 were located in the region −60 to −458 bp.

It has recently been reported that Sp1 may be involved in the genesis of steatosis and that other factors such as oxidative stress

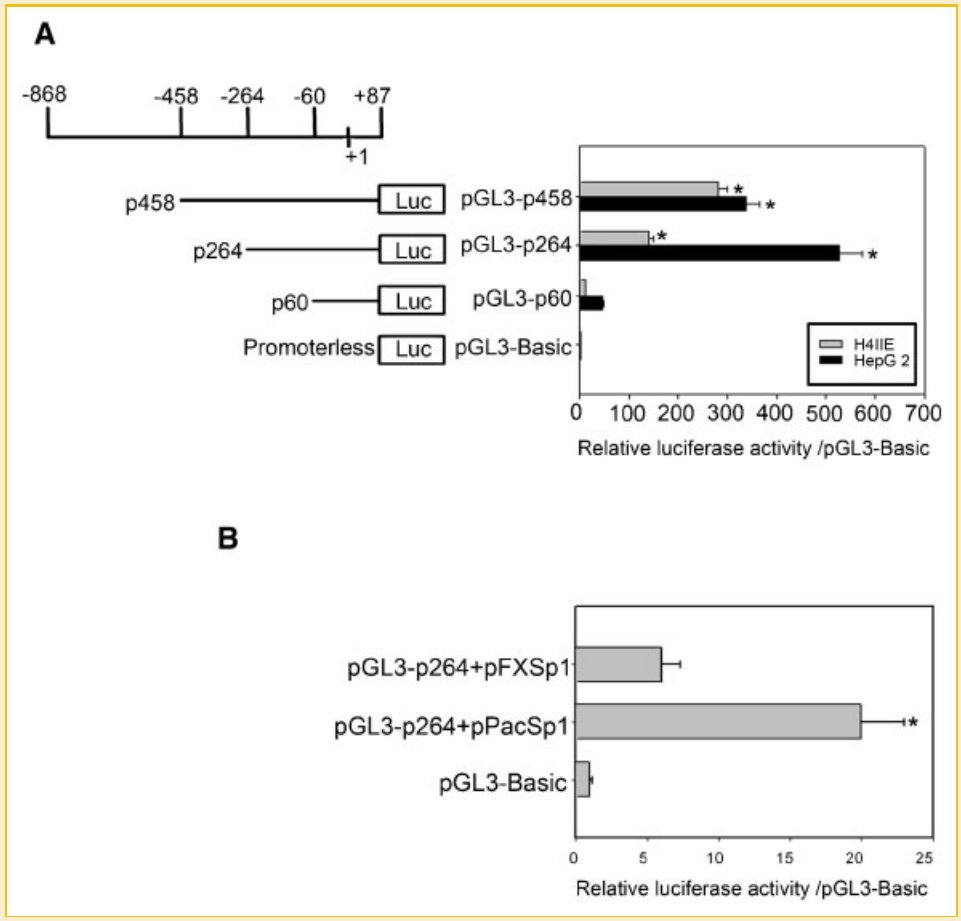

Fig. 2. Promoter activity of rat *ucp2*. A: Schematic representation of rat *ucp2* chimeric constructs. Progressive 5′-deletion of the rat *ucp2* promoter extending from −458 to −60 bp was generated by PCR (see Construction of Rat *ucp2* Promoter Luciferase Plasmids Section) and fused to the promoterless pGL3-Basic vector. Numbering was defined relative to the transcription start site. Graphical representation of luciferase activity in H4IIE and HepG2 cells transfected with the chimeric constructs. The pGL3-Basic vector was used as a negative control. Luciferase activities are expressed as fold induction over pGL3-Basic vector. The data represent the mean ± SD from three independent experiments. $^{*}P < 0.01$, compared with pGL3-p60 construct. B: Effect of transiently overexpressed Sp1 on the promoter activity of rat *ucp2*. Sp1 was co-transfected with pGL3-p264. The results depicted were the mean ± SD from three independent experiments. $^{*}P < 0.05$, compared with pGL3-p264 + pFXSp1 construct.

may trigger the progression of steatosis to NASH. To confirm the role of Sp1 on the regulation of *ucp2* transcription, pPacSp1 vector was co-transfected with PGL3-p264 into H4IIE cells. pFXSp1 vector, in which Sp1 is frame-shift mutated, was introduced as a negative control. The pPacSp1 and pFXSp1 vectors were provided by Engshang Huang, Chapel Hill, USA. Overexpression of Sp1 caused a ~300% increase in *ucp2* promoter activity compared with Sp1 negative control, indicating that Sp1 probably participates in the regulation of *ucp2* transcription (Fig. 2B).

IDENTIFICATION OF THE SP1 *cis*-ACTING ELEMENT THAT REGULATES RAT *ucp2* TRANSCRIPTION

The labeled probe (−84 to −61 bp) formed a band of DNA–protein complex after the addition of nuclear extracts of H4IIE cells (Fig. 3A, lane 1). This band vanished upon competition with 200-fold molar excess of unlabeled probe (lane 3), but could not be removed by competition with mutant Sp1 oligonucleotides (lane 2). The band of DNA–protein was supershifted by the addition of anti-Sp1 antibody (lane 4). EMSA results indicate that the Sp1 element in the proximal region upstream of the transcription start site has an important role in the regulation of *ucp2* promoter activity, at least in H4IIE cells.

ChIP—which is an alternative, in vivo method—was performed to elucidate whether Sp1 was factor bound to the promoter region. Nuclear DNA was extracted from the cells and subjected to PCR amplification with a pair of primers (−264/+87, Table I) of rat *ucp2* promoter. As a result, the band from the anti-Sp1 antibody pulling down DNA was successfully amplified, whereas Sp1-targeted genomic DNA was undetectable if no antibody was added in place of the anti-Sp1 antibody (data not shown). The specificity of ChIP assay for Sp1 was confirmed by simultaneous amplification of β-actin promoter as negative control (lower panel of Fig. 3B). The identity of PCR products was confirmed by cloning into a T/A vector and DNA sequencing. The results obtained in vivo using ChIP provide the supporting data for EMSA and supershift assay against Sp1 in vitro.

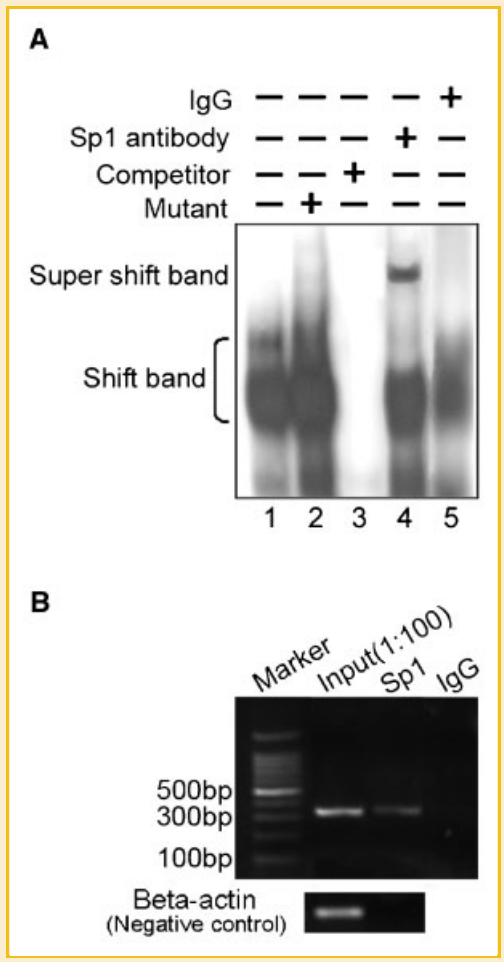

Fig. 3. Analysis of Sp1 *cis*-element in *ucp2* proximal promoter. A: EMSA for Sp1 binding to the *ucp2* promoter region from −84 to −61 bp. A DNA–protein complex was formed upon the addition of H4IIE nuclear extract (lane 1). Mutant Sp1 probe could not compete for this band (lane 2). However, this band was completely inhibited by excess unlabeled competitor (lane 3). The band was supershifted after the addition of 2 μg polyclonal anti-Sp1 antibody (lane 4). As a control for these experiments, the same reaction was performed with a nonimmunized rabbit IgG fraction (lane 5). B: ChIP assay in H4IIE cells showing that Sp1 can bind to the rat *ucp2* promoter site, as shown in (A). Amounts of co-precipitated DNA and the corresponding amounts in the input chromatin samples were measured by PCR. 15 μg of chromatin was immunoprecipitated with UCP2 antibody and an irrelevant antibody (IgG). The lane of input represented 1% of the total chromatin used in the ChIP assays. Thirty-five cycles of PCR were performed using specific primers as described in Chromatin Immunoprecipitation Assay (ChIP) Section, and products were run on a 2.0% agarose gel with ethidium bromide. Beta-actin promoter is included as a negative control (lower panel).

HEPATIC LESIONS AND EXPRESSION OF UCP2 IN RATS WITH NASH

We first generated an animal model, which closely resembles human NASH [Brunt et al., 1999]. After consumption of a high-fat diet for 12 weeks, it was found that serum levels of ALT and AST in the rats with NASH were moderately increased. The level of LDL increased about sevenfold as compared with the rats fed a standard diet. Glucose levels were also slightly increased in the rats with NASH. In addition, the liver index of rats fed a high-fat diet increased relative to controls (Table II). Histological examinations showed that livers

TABLE II. Liver Function Test

Groups	Control	NASH
ALT (U/L)	37.40 ± 8.36	81.10 ± 29.49*
AST (U/L)	101.30 ± 23.67	155.40 ± 75.31*
GLU (mmol/L)	9.31 ± 0.99	10.90 ± 1.51*
TG (mmol/L)	0.51 ± 0.12	0.54 ± 0.28
TC (mmol/L)	1.76 ± 0.32	2.05 ± 0.74
HDL (mmol/L)	1.34 ± 0.22	1.37 ± 0.43
LDL (mmol/L)	0.23 ± 0.45	1.65 ± 0.97*
Liver index (%)	2.53 ± 0.47	4.55 ± 0.61*

The liver index was calculated as the liver weight divided by the weight of the rat.
*Versus the control group $P < 0.05$.

of rats fed a high-fat diet have significant fat accumulation. The livers showed some microvesicular and mild macrovesicular steatosis localized in the periportal area and around the pericentral zone. Foci of lobular inflammation with liver-cell ballooning degeneration and necrosis appeared scattered throughout livers of the rats with NASH (Fig. 4A). Fat droplets in the hepatocytes were confirmed by oil red O staining (Fig. 4B). Masson's staining results indicated that perisinus fibrosis occurred only in the liver of rat with NASH (Fig. 4C). In the liver of rat with NASH, transmission electron microscopy analysis showed abnormal mitochondria with degenerative changes, including rarefied matrix and loss of cristae (Fig. 4D). These data indicate that livers of rats fed a high-fat diet develop hepatic lesions, dysfunction and hyperlipidemia.

Immunohistochemical staining revealed that lower levels of UCP2 were expressed in the hepatic cytoplasm of non-fatty liver (Fig. 5A), whereas expression levels were significantly higher in the livers of rats with NASH. Upregulation of UCP2 expression was also confirmed by Western blot (Fig. 5B). The results of real-time reverse transcription PCR analysis demonstrated that the expression of *ucp2* mRNA in the livers of animals with NASH was ~3.5-fold that in the livers of non-NASH animals (Fig. 5C).

SP1 BINDING TO THE *ucp2* PROMOTER IN THE LIVERS OF RATS WITH NASH

To identify the potential role of Sp1 in regulating UCP2 in the livers of rats with NASH, we performed EMSA using oligonucleotide probes that were the same as those applied in vitro. Briefly, one pM of oligonucleotide probe (corresponding to −84/−61 bp) was labeled with biotin. A total of 20 fM of the probe was added to the reaction mix containing 5 μg rat liver nuclear extract or H4IIE nuclear extract, 1 μl poly dI-dC and 2 μl 10× binding buffer (LightShiftTM chemiluminescent EMSA kit, Pierce Company). The reaction mixture was incubated for 20 min at room temperature. For supershift assays, 2 μg of polyclonal anti-Sp1 antibody was added to nuclear extracts and incubated on ice for 20 min prior to addition of the labeled probe. Twenty microliters of the reaction mix was loaded on a 6% polyacrylamide gel and analyzed by EMSA assay in 0.5× TBE buffer. The probe of Sp1 containing motif (−84/−61) was able to bind to the liver nuclear extracts of rats with NASH, forming a notable retarded band of DNA/protein. This band could be obviously competed upon the addition of excessive unlabeled probe (Fig. 6A). The supershifted band of DNA–protein was visualized clearly following the addition of anti-Sp1 antibody (Fig. 6A).

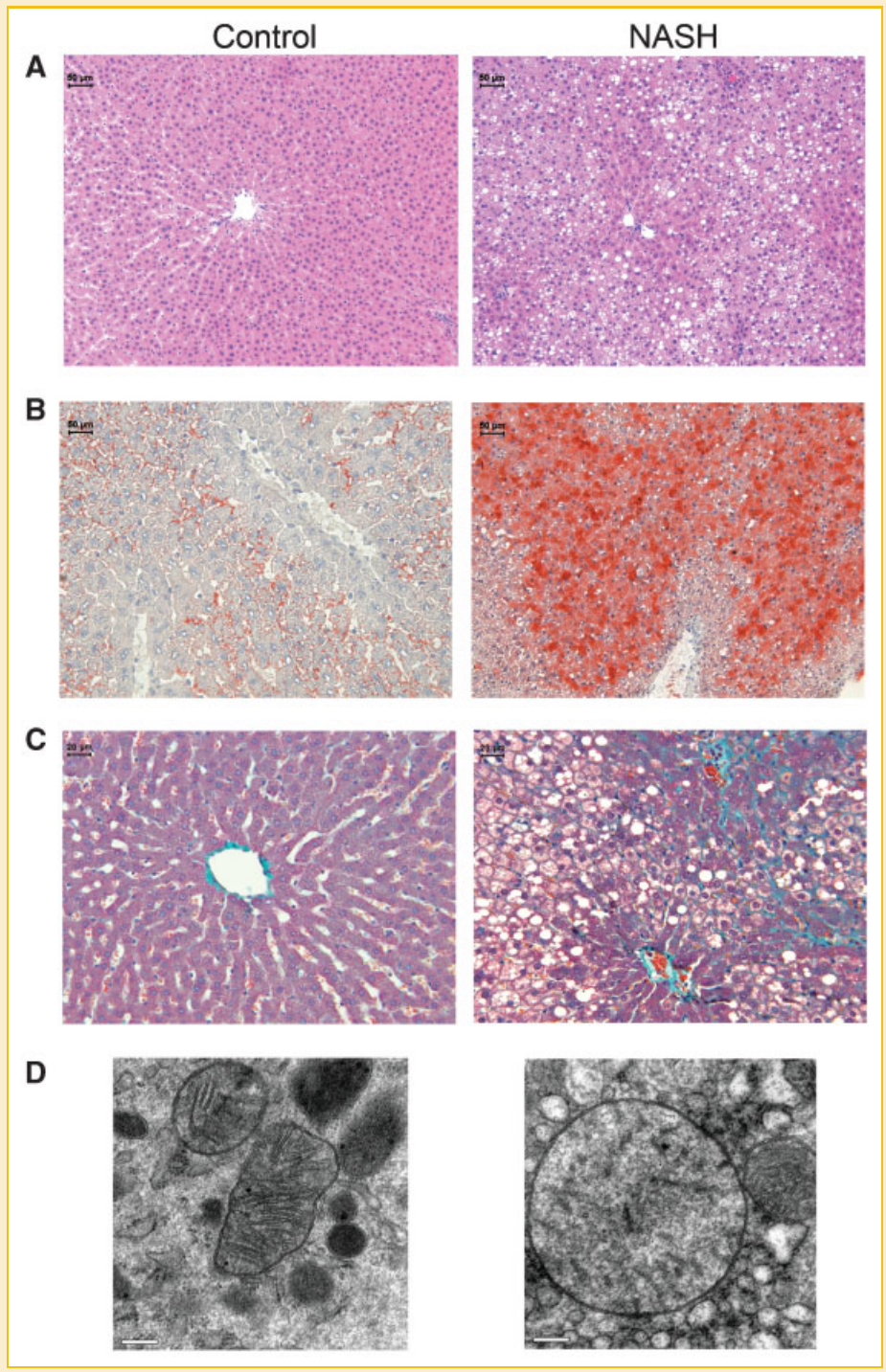

Fig. 4. Hepatic histology in rats fed a high-fat diet ad libitum. A: The liver samples were stained with hematoxylin and eosin (objective 10×). The livers of rats fed a standard diet show minimal mononuclear inflammatory cells (left). The livers of the rats fed a high-fat diet show pronounced hepatic steatosis, mononuclear inflammatory cells infiltrate and liver-cell necrosis. The hepatocytes show ballooning degeneration (right). B: Oil red O stain (objective 10×). The accumulation of fat droplets in hepatocytes was demonstrated by fat stain (red) on frozen tissue (right). The livers of rats fed a standard diet show minimal fat (left). C: Masson trichroma stain (objective 20×). In control rat livers, low amounts of collagen (blue) were detected predominantly around the central veins (left). Highlight collagen reveals mild fibrosis of the terminal hepatic vein and radiating pericellular (Disse space) fibrosis in the livers of NASH rats (right). D: Electron microscopy of hepatic mitochondria. Mitochondria in rats fed a high-fat diet ad libitum (right) show degenerative changes with rarefied matrix and loss of cristae. The hepatocyte mitochondria in rats fed a standard diet (left). The magnification is 60,000×.

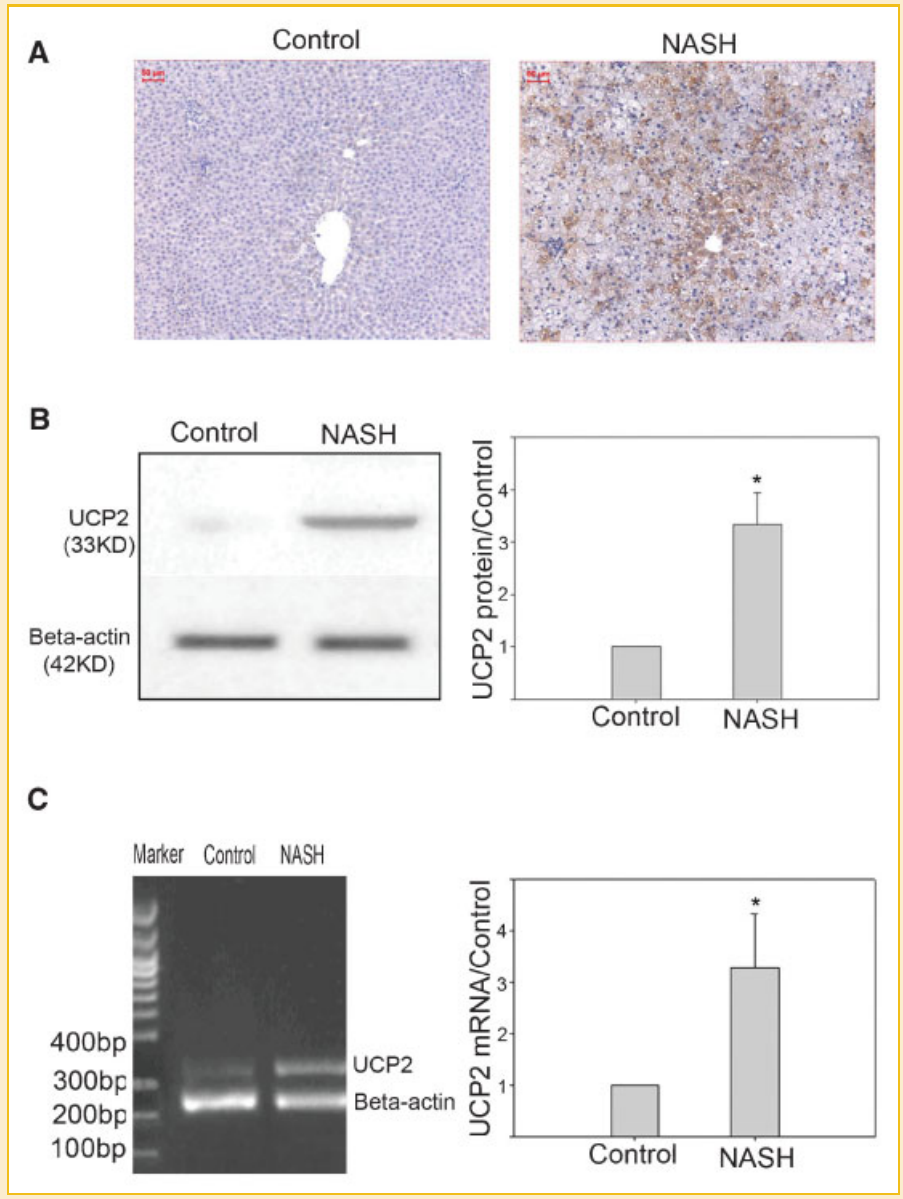

Fig. 5. UCP2 expression in rat liver. The expression of UCP2 protein and mRNA was analyzed using immunohistochemistry, Western blot and real-time PCR. Data shown are the means of six independent experiments in which $P < 0.05$ versus control rats. A: Immunohistochemical staining of UCP2 in normal or nonalcoholic steatohepatitis (NASH) rat liver. In normal rat liver, lower levels of UCP2 are expressed in the hepatic cytoplasm around the central vein, but this protein is ubiquitously expressed in the hepatic cytoplasm of rats with NASH. B: Western blot analysis of hepatic UCP2 expression. One hundred micrograms of protein extract from the livers of rats with NASH—which are prepared by being fed a high-fat diet for 12 weeks—was separated by 12% SDS–PAGE and probed with antibody against UCP2. UCP2 protein expression was normalized to β-actin. Results quantified under the blots are the average values of two representative blots per sample. C: Real-time PCR was carried out to determine the fold difference in UCP2 mRNA expression between normal and fatty livers. UCP2 mRNA expression was normalized to β-actin. Asterisks indicate a statistically significant difference from controls, $P < 0.05$, by ANOVA.

Given its ability to bind in vitro, we attempted to confirm that Sp1 binds to the rat *ucp2* proximal promoter in vivo, particularly under NASH conditions. To accomplish this, liver sections from rats with NASH or non-fatty liver were cross-linked with formaldehyde and subjected to ChIP analysis. In non-fatty liver (control), it was indicated that Sp1 could bind to −84/−61 elements of the *ucp2* promoter to a small extent; however, in the case of NASH liver, the level of Sp1 binding was increased (Fig. 6B).

The binding of Sp1 to its site in the *ucp2* gene promoter was confirmed by ChIP analysis. As shown in Figure 6B, PCR amplification of the Sp1-ChIP product (−264/+87) of the *ucp2* gene produced a band (lane 3 from control, lane 6 from NASH). However, no bands could be amplified using β-actin primers as a

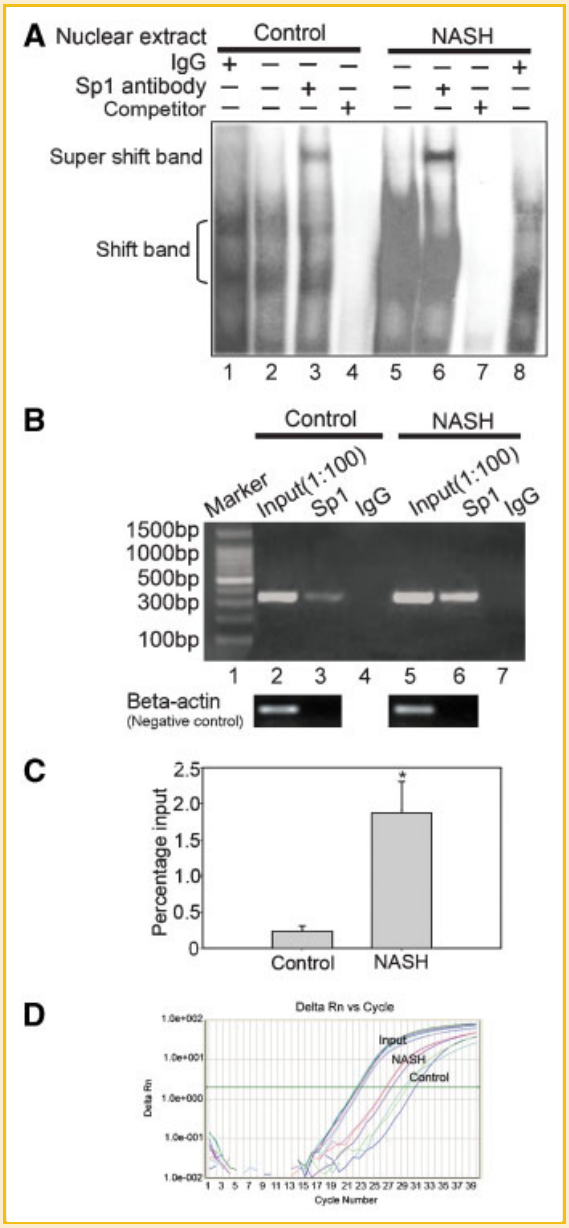

Fig. 6. In vitro and in vivo assay of Sp1 binding to *ucp2* proximal promoter in rat liver. A: EMSA was performed by incubating liver nuclear extracts from normal and fatty rat liver tissue with probe (−84 to −61 bp) in the presence or absence of specific competitors (unlabeled probe) and anti-Sp1 antibody. B: ChIP assay of Sp1 bound to rat *ucp2* promoter. Liver pieces from control rats and rats with NASH were cross-linked in 1% formaldehyde. Chromatin was extracted and fragmentized with sonication to an average size of 200–600 bp. 15 μg of chromatin was immunoprecipitated with UCP2 antibody. The precipitation was amplified by PCR for 25 cycles using specific primers, as indicated in Table I, and the products were run on a 2.0% agarose gel with ethidium bromide. An irrelevant antibody (IgG) was added as input control. Beta-actin promoter was included as a negative control (lower panel). C,D: Real-time PCR of ChIPed DNA in samples of NASH and control livers. The relative differences between the input sample and Sp1 were determined using the ΔCT method (see Materials and Methods Section). These values were presented as percentage inputs in which the DNA reverse-cross-linked input sample was taken as 100%. Data were the mean ± SD from triplicate samples of three independent experiments. $^{*}P < 0.01$, compared with control group. [Color figure can be viewed in the online issue, which is available at www.interscience.wiley.com.]

negative control (lower panel, Fig. 6B), demonstrating the specificity of the Sp1-ChIP product. Therefore, we confirmed that Sp1 can bind the *ucp2* promoter at the −84/−61 site predicted by our gel-shift analysis of the livers of rats with NASH (Fig. 6A).

To quantify the ChIP results showing an increase in Sp1 binding, real-time PCR was performed (Fig. 6C/D). The relative quantity of Sp1-ChIP DNA in non-fatty liver sample was 0.24% of the quantity of input control DNA; however, this value was increased to 1.87% in NASH-liver samples, an increase of nearly 7.7-fold. The results of quantitative real-time PCR indicate that Sp1 can bind the proximal promoter of *ucp2*, the binding of which is increased during NASH.

DISCUSSION

Precious control of mouse *ucp2* transcription has been extensively studied by Medvedev et al. [2001, 2002] during observation of the response of rat-derived INS-1 pancreatic beta cells to free fatty acid (FFA) or the response of preadipocytes to PPARγ stimulation. These authors reported that an enhancer region (−86/−44) seems to be crucial because deletion of this fragment would not only result in reduction of the basal promoter activity, but also eliminate response of the *ucp2* gene to specific stimulation by FFA or PPARγ. Obviously, this enhancer region contains several potential binding sites for Sp1, sterol regulatory element (SRE) and E-Box. Of the three *cis*-elements, SRE and E-Box have been shown to be the main modulators of *ucp2* transcription. The role of Sp1 on regulation of *ucp2* transcription seemed also important. Mutation of Sp1 site resulted in nearly 70% reduction in *ucp2* promoter activity. However, whether these factors are related to fatty liver, particularly its coordinated contribution to pathogenesis of NASH remains unclear. Here, we aimed to investigate Sp1-regulated *ucp2* transcription in the livers of rats with NASH. In the present study, a 0.5-kb fragment of the rat *ucp2* proximal promoter was isolated and the promoter activity was analyzed using reporter assay, gel shift and ChIP. In particular, potential consensus Sp1-binding sites in the 5′-flanking region near to the transcription start site were investigated. Classical regulatory elements such as TATA and CAAT boxes do not exist in the rat *ucp2* proximal promoter; instead, GC-rich binding elements such as Sp1 and E-box motifs are located in the proximal promoter, which is identical to the mouse *ucp2* promoter [Yamada et al., 1998]. It was reported that the region between nucleotide −233 and −34 in the mouse *ucp2* promoter revealed particularly strong enhancer activity [Yoshitomi et al., 1999]. An 80-bp fragment (−141 to −66) in the human *ucp2* promoter was considered to be a critical element for promoter activity and tissue specificity [Tu et al., 1998].

The promoter assay in the present study demonstrated that removal of the fragment from −458 to −264 bp led to a notable change in promoter activity in two cell lines. In HepG2 cells, this fragment seems to regulate *ucp2* transcription negatively, whereas it seems to function as a positive regulator in H4IIE cells (Fig. 2). So far, we cannot find a reasonable explanation. Further study is required to clarify whether the results are due to differential response of the cell lines (H4IIE and HepG2) to Sp1 factor. However,

deletion of the fragment from −264 to −60 bp led to a significant and consistent decrease in promoter activities in both cells, indicating that there exists a functionally regulatory *cis*-acting element in this region. It is well known that Sp1 can regulate the expression of many genes associated with fatty acid metabolism. We next investigated whether the enhancement of *ucp2* promoter activity is attributable to removal of the Sp1-containing fragment (from −264 to −60 bp). We found that a putative Sp1-binding site (a GC-rich element with a core sequence of CCCGCC −83 to −78 nt) might be crucial for basal promoter activity (Fig. 3A). Subsequently, we used ChIP assay, which is a more reliable strategy than other in vitro methods such as EMSA, and obtained a supporting data to further confirm the interactive ability of transcriptional factor Sp1 to bind *ucp2* promoter (Fig. 3B). Increasing the exogenous cellular Sp1 content by introducing an Sp1-expressing vector confirmed the ability of Sp1 to bind to its motif (−83 to −78 nt) in the *ucp2* promoter of H4IIE cells, thereby increasing promoter activity (Fig. 2B).

Sp1 is a member of a family of zinc-finger transcription factors that includes at least four Sp proteins [Black et al., 1999, 2001; Suske, 1999]. These transcription factors have important roles in many physiological processes, including cell-cycle regulation, hormonal activation, apoptosis and angiogenesis. Sp proteins share several well-conserved functional domains such as the N-terminal transcription activation domain and the C-terminal zinc-finger DNA-binding domain [Kadonaga et al., 1987, 1988; Courey and Tjian, 1988; Courey et al., 1989]. It has been reported that Sp1, even bound to the distal promoter, strongly influence other transcription factor bound to proximal elements of the promoter. For example, Spl bound 1,700 nucleotides downstream of the RNA start site of the herpes simplex virus thymidine kinase gene can act synergistically with the factor bound at the normal upstream position at −100 [Courey et al., 1989]. Using electronic microscope Mastrangelo et al. [1991] conclude this phenomenon as direct consequence of interactions between remote and local Sp1, the remote Spl translocated to the promoter by a DNA loop. Sp1 has an important role in the transcriptional activation of many genes, including those essential to fatty acid metabolism such as the gene encoding the insulin receptor [Fukuda et al., 2001] and those encoding rate-limiting enzymes in the biosynthesis of fatty acids (e.g., low-density lipoprotein receptor, acetyl-CoA carboxylase and fatty acid syntheses [Fukuda et al., 1997; Ikeda et al., 2001]). Sp1 is widely expressed in various tissues and binds to GC-box motifs in promoters. It is considered to be an essential element in the sterol regulation of the rat fatty acid synthase gene [Wolf et al., 2001]. Prior to binding to the corresponding motif, Sp1 must be post-translationally modified by glycosylation [Roos et al., 1997] and phosphorylation [Black et al., 1999].

In rats, *ucp2* is mapped on chromosome 1, and abnormal UCP2 expression was found in rats with glucose intolerance and adiposity in type II diabetes [Fleury et al., 1997; Chan et al., 1999; Zhang et al., 2001]. Many situations or factors such as a hyperlipidemic diet, starvation, obesity, free fatty acids, leptin, thiazolidinediones, thyroid hormones, endotoxin and phorbol ester also modulate *ucp2* transcription or expression in various tissues or cell types [Krauss et al., 2005]. However, to our knowledge, ours is the first attempt to examine the effect of Sp1 on rat liver *ucp2* expression in animals with NASH.

In this study, the liver histopathology of rats fed a high-fat diet ad libitum showed typical hepatic lesion associated with NASH: steatosis, inflammation and early fibrosis. Chronically, because excessive fat accumulation in the liver may be a predisposing condition for hepatic inflammation, steatohepatitis and liver cirrhosis (which leads to death [Matteoni et al., 1999]), efforts are required to prevent fatty liver damage. In our investigation of UCP2 expression and its possible relationship with Sp1 during the accumulation of fat in liver, we observed a 3.5-fold increase in the expression of *ucp2* mRNA in the livers of rats with NASH compared with rats without NASH (Fig. 5). Furthermore, we showed that the expression of Sp1 and its increased binding capacity have an important role in the pathogenesis of NASH in rats. A recent study reported that Sp1 was hyperphosphorylated at serine residues in the livers of MAT1A-knockout mice [Rubio et al., 2007]. The authors reported that the level of Sp1 phosphorylation on serine but not threonine residues was markedly increased in MAT1A-KO livers, whereas the total hepatic Sp1 content remained unchanged. Moreover, Sp1 phosphorylation on serine residues was slightly increased in liver samples from patients with NASH and steatosis compared with subjects with normal hepatic function, suggesting that activation of Sp1 may have a role in pathogenesis of steatosis and NASH. The finding that Sp1 is hyperphosphorylated in both steatosis and NASH could strongly support our present study.

In conclusion, the present study addresses the important role of Sp1 regulation on *ucp2* transcription in rat hepatic cells and in the livers of rats with NASH. In this article, we have presented the first evidence that Sp1 is directly involved in the transcription of rat *ucp2* in H4IIE cells. The livers of rats with NASH expressed higher levels of UCP2 than did the livers of rats without NASH, which we attribute to the regulation of Sp1 bound to the *ucp2* promoter.

ACKNOWLEDGMENTS

This work was supported by the National Natural Science Foundation of China (No. 30470643), the National "863" Project (2006AA02A410) and Beijing Municipal Commission of Education. We are grateful to Ms. Zeng XB and Sun HM for their preparation of histological slides. We also thank Mr. Guo D for his assistance of figure preparation.

REFERENCES

Baffy G. 2005. Uncoupling protein-2 and non-alcoholic fatty liver disease. Front Biosci 10:2082–2096.

Black AR, Jensen D, Lin SY, Azizkhan JC. 1999. Growth/cell cycle regulation of Sp1 phosphorylation. J Biol Chem 274:1207–1215.

Black AR, Black JD, Zizkhan-Clifford J. 2001. Sp1 and kruppel-like factor family of transcription factors in cell growth regulation and cancer. J Cell Physiol 188:143–160.

Brunt EM, Janney CG, Di Bisceglie AM, Neuschwander-Tetri BA, Bacon BR. 1999. Nonalcoholic steatohepatitis: A proposal for grading and staging the histological lesions. Am J Gastroenterol 94:2467–2474.

Caldwell SH, Oelsner DH, Iezzoni JC, Hespenheide EE, Battle EH, Driscoll CJ. 1999. Cryptogenic cirrhosis: Clinical characterization and risk factors for underlying disease. Hepatology 29:664–669.

Chakravarty K, Wu SY, Chiang CM, Samols D, Hanson RW. 2004. SREBP-1c and Sp1 Interact to regulate transcription of the gene for phosphoenolpyruvate carboxykinase (GTP) in the liver. J Biol Chem 279:15385–15395.

Chan CB, MacDonald PE, Saleh MC. 1999. Overexpression of uncoupling protein 2 inhibits glucose-stimulated insulin secretion from rat islets. Diabetes 48:1482–1486.

Clark JM, Brancati FL, Diehl AM. 2002. Nonalcoholic fatty liver disease. Gastroenterology 122:1649–1657.

Cortez-Pinto H, Yang SQ, Lin HZ, Costa S, Hwang CS, Lane MD, Bagby G, Diehl AM. 1998. Bacterial lipopolysaccharide induces uncoupling protein-2 expression in hepatocytes by a tumor necrosis factor-alpha-dependent mechanism. Biochem Biophys Res Commun 251:313–319.

Courey AJ, Tjian R. 1988. Analysis of Sp1 *in vivo* reveals multiple transcriptional domains including a novel glutamine-rich activation motif. Cell 55:887–898.

Courey AJ, Holtzman DA, Jackson SP, Tjian R. 1989. Synergistic activation by the glutamine-rich domains of human transcription factor Sp1. Cell 59:827–836.

Day CP. 2002. Non-alcoholic steatohepatitis (NASH): Where are we now and where are we going? Gut 50:585–588.

Farrell GC, Chitturi S, Lau GKK, Sollano JD. 2007. Guidelines for the assessment and management of non-alcoholic fatty liver disease in the Asia-Pacific region: Executive summary. J Gastroen Hepatol 22:775–777.

Fleury C, Neverova M, Collins S, Raimbault S, Champigny O, LeviMeyrueis C, Bouillaud F, Seldin MF, Surwit RS, Ricquier D, Warden CH. 1997. Uncoupling protein-2: A novel gene linked to obesity and hyperinsulinemia. Nat Genet 15:269–272.

Fromenty B, Robin MA, Igoudjil A, Mansouri A, Pessayre D. 2004. The ins and outs of mitochondrial dysfunction in NASH. Diabetes Metab 30:121–138.

Fukuda H, Iritani N, Noguchi T. 1997. Transcriptional regulatory regions for expression of the rat fatty acid synthase. FEBS Lett 406:243–248.

Fukuda H, Noguchi T, Iritani N. 2001. Transcriptional regulation of insulin receptor gene promoter in rat hepatocytes. Biochem Biophys Res Commun 280:1274–1278.

Gummow BM, Winnay JN, Hammer GD. 2003. Convergence of Wnt signaling and steroidogenic factor-1 (SF-1) on transcription of the rat inhibin alpha gene. J Biol Chem 278:26572–26579.

Hidaka S, Kakuma T, Yoshimatsu H, Yasunaga S, Kurokawa M, Sakata T. 1998. Molecular cloning of rat uncoupling protein 2 cDNA and its expression in genetically obese Zucker fatty (fa/fa) rats. Biochim Biophys Acta 1389:178–186.

Ikeda Y, Yamamoto J, Okamura M, Fujino T, Takahashi S, Takeuchi K, Osborne TF, Yamamoto TT, Ito S, Sakai J. 2001. Transcriptional regulation of the murine acetyl-CoA synthetase 1 gene through multiple clustered binding sites for sterol regulatory element-binding proteins and a single neighboring site for Sp1. J Biol Chem 276:34259–34269.

Kadonaga JT, Carner KR, Masiarz FR, Tjian R. 1987. Isolation of cDNA encoding transcription factor Sp1 and functional analysis of the DNA binding domain. Cell 51:1079–1090.

Kadonaga JT, Courey AJ, Ladika J, Tjian R. 1988. Distinct regions of Sp1 modulate DNA binding and transcriptional activation. Science 242:1566–1570.

Kaisaki PJ, Woon PY, Wallis RH, Monaco AP, Lathrop M, Gauguier D. 1998. Localization of *tub* and uncoupling proteins (*Ucp*) 2 and 3 to a region of rat chromosome 1 linked to glucose intolerance and adiposity in the Goto-Kakizaki (GK) type 2 diabetic rats. Mamm Genome 9:910–912.

Krauss S, Zhang CY, Lowell BB. 2005. The mitochondrial uncoupling-protein homologues. Nat Rev Mol Cell Biol 6:248–261.

Lagor WR, de Groh ED, Ness GC. 2005. Diabetes alters the occupancy of the hepatic 3-hydroxy-3-methylglutaryl-CoA reductase promoter. J Biol Chem 280:36601–36608.

Larrouy D, Laharrague P, Carrera G, ViguerieBascands N, LeviMeyrueis C, Fleury C, Pecqueur C, Nibbelink M, Andre M, Casteilla L, Ricquier D. 1997. Kupffer cells are a dominant site of uncoupling protein 2 expression in rat liver. Biochem Biophys Res Commun 235:760–764.

Lowry O, Rosebrough NJ, Farr AL, Randal RJ. 1951. Protein measurements with the Folin phenol reagent. J Biol Chem 193:265–275.

Ludwig J, Viggiano TR, McGill DB, Oh BJ. 1980. Nonalcoholic steatohepatitis: Mayo clinic experiences with a hitherto unnamed disease. Mayo Clin Proc 55:434–438.

Mastrangelo IA, Courey AJ, Wall JS, Jackson SP, Hough P. 1991. DNA looping and SpI multimer links: A mechanism for transcriptional synergism and enhancement. Proc Natl Acad Sci 88:5670–5674.

Matsuda J, Hosoda K, Itoh H, Son C, Doi K, Tanaka T, Fukunaga Y, Inoue G, Nishimura H, Yoshimasa Y, Yamori Y, Nakao K. 1997. Cloning of rat uncoupling protein-3 and uncoupling protein-2 cDNAs: Their gene expression in rats fed high-fat diet. FEBS Lett 418:200–204.

Matteoni CA, Younossi ZM, Gramlich T, Boparai N, Liu YC, McCullough AJ. 1999. Nonalcoholic fatty liver disease: A spectrum of clinical and pathological severity. Gastroenterology 116:1413–1419.

Medvedev AV, Snedden SK, Raimbault S, Ricquier D, Collins S. 2001. Transcriptional regulation of the mouse uncoupling protein-2 gene. Double E-box motif is required for peroxisome proliferator-activated receptor-gamma-dependent activation. J Biol Chem 276:10817–10823.

Medvedev AV, Robidoux J, Bai X, Cao WH, Floering LM, Daniel KW, Collins S. 2002. Regulation of the uncoupling protein-2 gene in INS-1 beta-cells by oleic acid. J Biol Chem 277:42639–42644.

Neuschwander-Tetri BA, Caldwell SH. 2003. Nonalcoholic steatohepatitis: Summary of an AASLD Single Topic Conference. Hepatology 37:1202–1219.

Ou XM, Chen K, Shih JC. 2004. Dual functions of transcription factors, transforming growth factor β-inducible early gene (TIEG)2 and Sp3, are mediated by CACCC element and Sp1 sites of human monoamine oxidase (MAO) B gene. J Biol Chem 279:21021–21028.

Pecqueur C, Cassard-Doulcier AM, Raimbault S, Miroux B, Fleury C, Gelly C, Bouillaud F, Ricquier D. 1999. Functional organization of the human uncoupling protein-2 gene, and juxtaposition to the uncoupling protein-3 gene. Biochem Biophys Res Commun 255:40–46.

Pecqueur C, ves-Guerra MC, Gelly C, Levi-Meyrueis C, Couplan E, Collins S, Ricquier D, Bouillaud F, Miroux B. 2001. Uncoupling protein 2, *in vivo* distribution, induction upon oxidative stress, and evidence for translational regulation. J Biol Chem 276:8705–8712.

Pessayre D, Fromenty B. 2005. NASH: A mitochondrial disease. J Hepatol 42:928–940.

Ricquier D, Bouillaud F. 1997. The mitochondrial uncoupling protein: Structural and genetic studies. Prog Nucleic Acid Res Mol Biol 56:83–108.

Roos MD, Su KH, Baker JR, Kudlow JE. 1997. *O* glycosylation of a Sp1-derived peptide blocks known Sp1 protein interactions. Mol Cell Biol 17:6472–6480.

Rubio A, Guruceaga E, Vazquez-Chantada M, Sandoval J, Martinez-Cruz LA, Segura V, Sevilla JL, Podhorski A, Corrales FJ, Torres L, Rodriguez M, Aillet F, Ariz U, Arrieta FM, Caballeria J, Martin-Duce A, Lu SC, Martinez-Chantar ML, Mato JM. 2007. Identification of a gene-pathway associated with non-alcoholic steatohepatitis. J Hepatol 46:708–718.

Samaras SE, Cissell MA, Gerrish K, Wright CVE, Gannon M, Stein R. 2002. Conserved sequences in a tissue-specific regulatory region of the *pdx*-1 gene

mediate transcription in pancreatic cells: Role for hepatocyte nuclear factor 3 and Pax6. Mol Cell Biol 22:4702–4713.

Sauzeau V, Rolli-Derkinderen M, Marionneau C, Loirand G, Pacaud P. 2003. RhoA expression is controlled by nitric oxide through cGMP-dependent protein kinase activation. J Biol Chem 278:9472–9480.

Schmittgen TD, Zakrajsek BA, Mills AG, Gorn V, Singer MJ, Reed MW. 2000. Quantitative reverse transcription-polymerase chain reaction to study mRNA decay: Comparison of endpoint and real-time methods. Anal Biochem 285:194–204.

Suske G. 1999. The Sp-family of transcription factors. Gene 238:291–300.

Tu N, Chen H, Winnikes U, Reinert I, Marmann G, Pirke KM, Lentes KU. 1998. Structural organization and mutational analysis of the human uncoupling protein-2 (hUCP2) gene. Life Sci 64:PL41–PL50.

Wolf SS, Roder K, Schweizer M. 2001. Role of Sp1 and Sp3 in the transcriptional regulation of the rat fatty acid synthase gene. Arch Biochem Biophys 385:259–266.

Yamada M, Hashida T, Shibusawa N, Iwasaki T, Murakami M, Monden T, Satoh T, Mori M. 1998. Genomic organization and promoter function of the mouse uncoupling protein 2 (UCP2) gene. FEBS Lett 432:65–69.

Yoshitomi H, Yamazaki K, Tanaka I. 1999. Mechanism of ubiquitous expression of mouse uncoupling protein 2 mRNA control by *cis*-acting DNA element in 5′-flanking region. Biochem J 340:397–404.

Zhang CY, Baffy G, Perret P, Krauss S, Peroni O, Grujic D, Hagen T, Vidal-Puig AJ, Boss O, Kim YB, Zheng XX, Wheeler MB, Shulman GI, Chan CB, Lowell BB. 2001. Uncoupling protein-2 negatively regulates insulin secretion and is a major link between obesity, cell dysfunction, and type 2 diabetes. Cell 105:745–755.